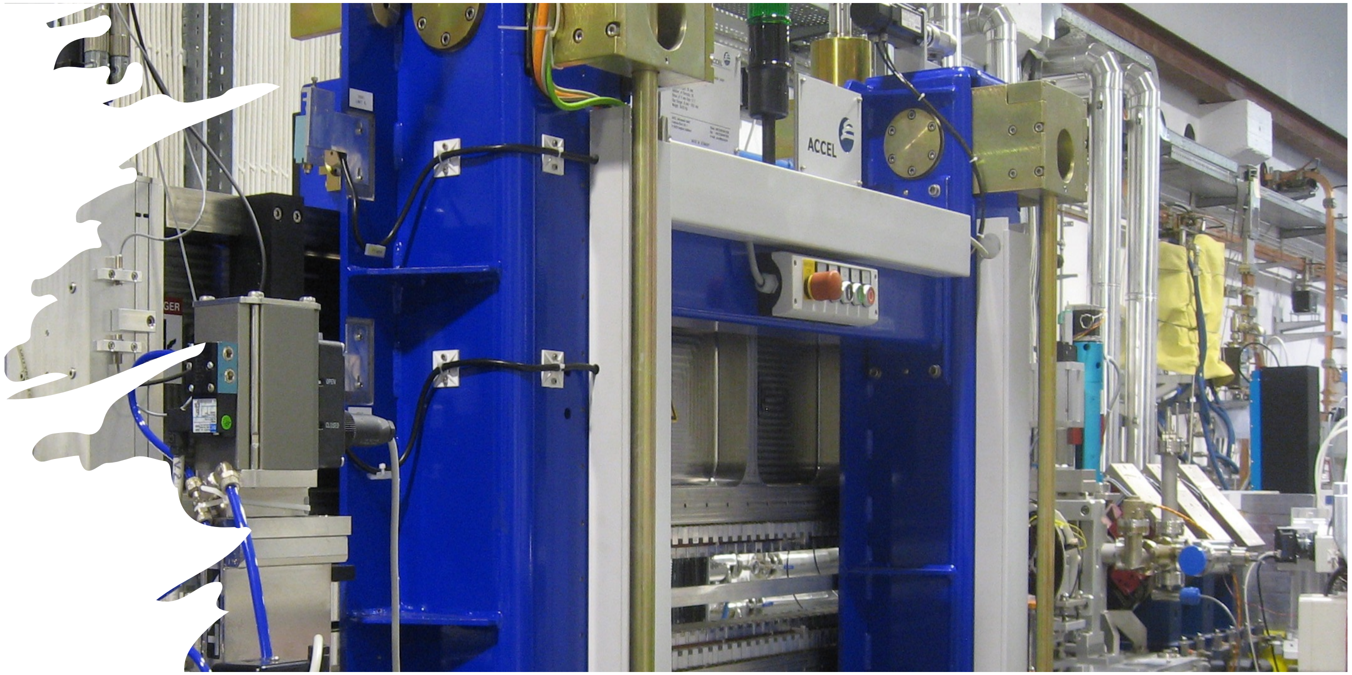

WA6 Report
FEL & Undulators

L. Giannessi (LNF),

on behalf of the WA6 collaboration team

A. Doria, M. Carpanese, F. Nguyen, A. Petralia (ENEA),

I. Balossino, M. Del Franco, M. Galletti, A. Giribono, A. Ghigo, A. Iovine, M. Opromolla, L. Sabbatini, A. Selce, C. Vaccarezza, A. Vannozzi, F. Villa, M. Castellano (Laboratori Nazionali di Frascati),

Vittoria Petrillo (Un. Milano),

Cristian Boffo (FNAL),

Najmeh Mirian (DESY)

Support from ***ENEA - Holographyc Interferometry & Fibre Optic Sensors (HIFOS) Laboratory*** *(M. Caponero, A. Polimadei)*

Outline

- **ARIA**
    - Undulators
    - Seed laser
    - Tuning range

VUV seeded HGHG FEL

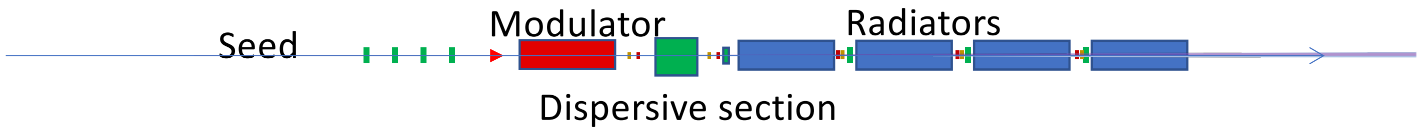

- **AQUA**
  - Magnetic design & tuning range
  - Vacuum chamber
  - Longitudinal and transverse Wake field analysis
  - Analysis of SABINA Undulator and first lessons for the AQUA undulator
    - **Magnetic:** field quality, field integrals, trajectory and FEL amplification
    - **Mechanical:** stability and reproducibility tests

Soft-X ray SASE FEL – optimized for 4 nm

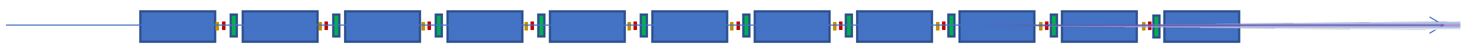

ARIA

Undulators, seed and tuning range

ARIA
Radiator Undulators

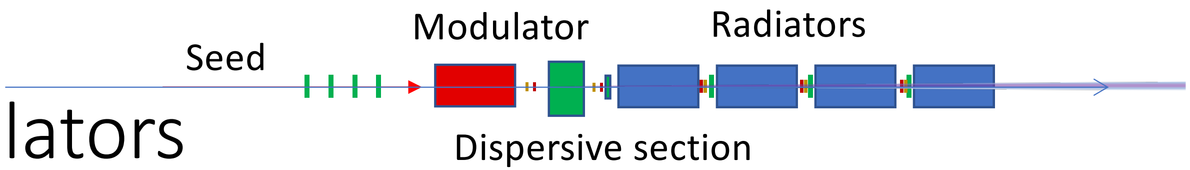

Main features:

- variable gap, variable phase for adjustable polarization (EPU) (six motors)
- λ_u = 55.2 mm, Np=42, L_u=2.4 m
- working gap: 10 ÷ 32 mm

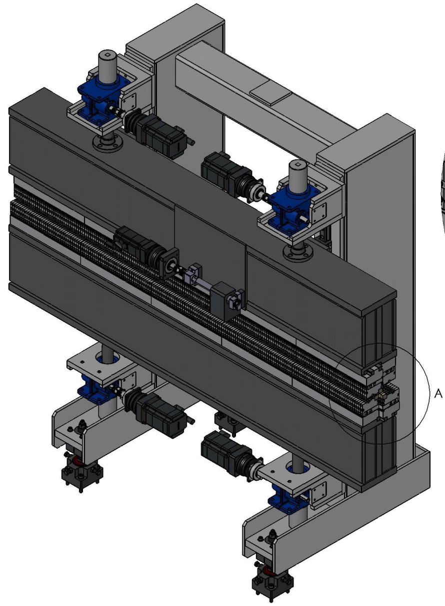

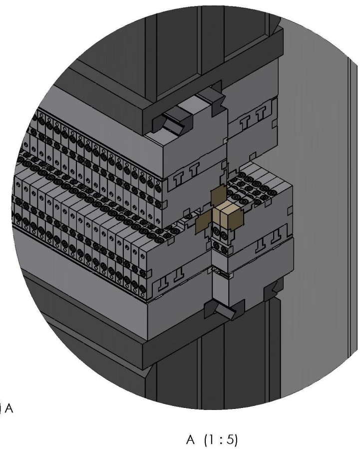

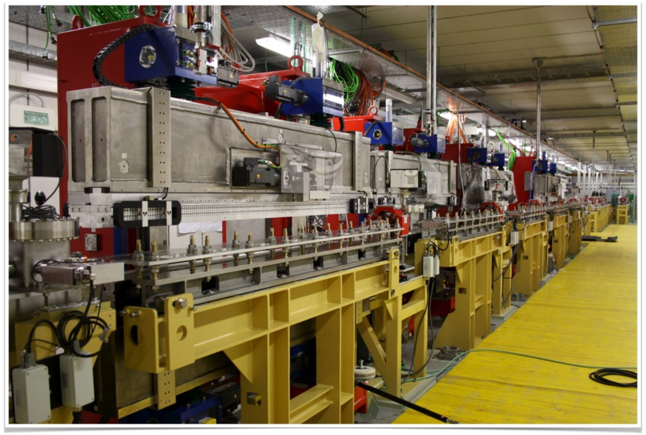

Similar to FERMI FEL-1 radiators built by KYMA in 2009-2010 for FERMI FEL-1

Main Physical Specifications:

Phase error σ_Φ	< 5 º rms
• Trajectory offset error	< 20 μm rms
• Trajectory tilt error	< 25 μrad rms
• Peak-to-peak field error ΔB/B	< 0.5% rms
• Integrated Quadrupole (N/S)	< 100 G
• Integrated Sextupole (N/S)	< 100 G/cm

Courtesy of Bruno Diviacco

ARIA Tuning range parameters

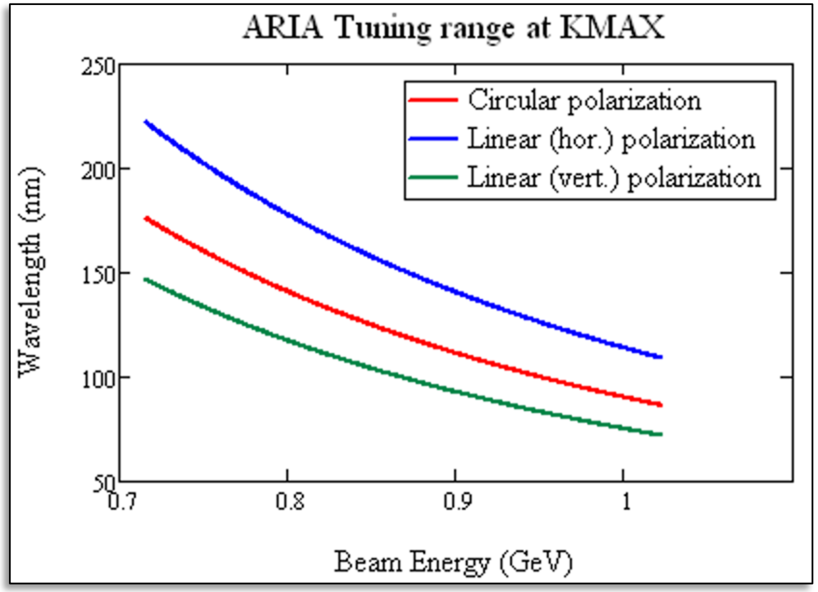

- **FEL**
  - Max harmonic = 10
  - Undulator K-range from FERMI FEL-1:

    K_{max} = 3.4 (CR), 4.35 (LV), 5.45 (LH)
- **Electron beam parameters:**
  - Energy 1.0 -> 0.7 GeV
  - Energy spread 200 keV @ 0.8 kA -> 400 keV@1.5 kA
  - e-beam duration:
    - > 100 fs (long bunch mode, 200 pC)
    - -> 8 fs (short bunch mode, 30 pC)
  - beam emittance 2 mm mrad in long bunch mode/ 0.8 mm mrad in short bunch mode - beta function 10 m
- **Seed laser:**
  - We assume a **minimum seed energy** available in the range, of **20 uJ**
  - The seed spot size (average) is independent on the wavelength and is **0.5 mm^2**
  - Seed duration **400 fs** (long seed) -> **200 fs** (short seed), possibly no frequency chirp – i.e. seed spectral width close to FTL (not essential in short bunch mode)

ARIA Seed laser option

https://lightcon.com/product/topas-prime-opa/#performance

INFN
Istituto Nazionale di Fisica Nucleare

Courtesy of M. Galletti

TOPAS | PRIME

Collinear Optical Parametric Amplifier

- 189 nm – 20 µm tuning range
- Up to 5 mJ pump pulse energy
- > 25% conversion efficiency
- High output stability
- CEP stabilization of Idler
- Fresh pump channel for improved temporal and spatial properties of sum-frequency options

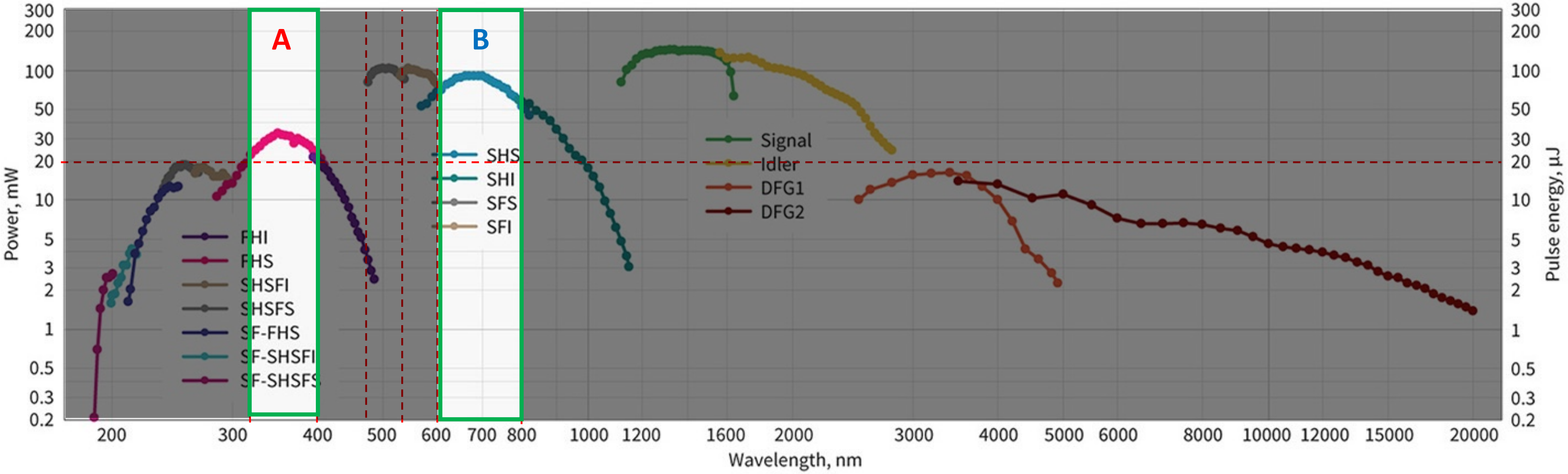

TOPAS-PRIME tuning curves. Pump: 1 mJ, 100 fs, 800 nm. HE version is commercial and E>10 uJ for the entire BW.

Long-bunch long-seed mode Linear Polarization

A: Seed range 320-400 nm

High energy range 100-50 nm – higher power

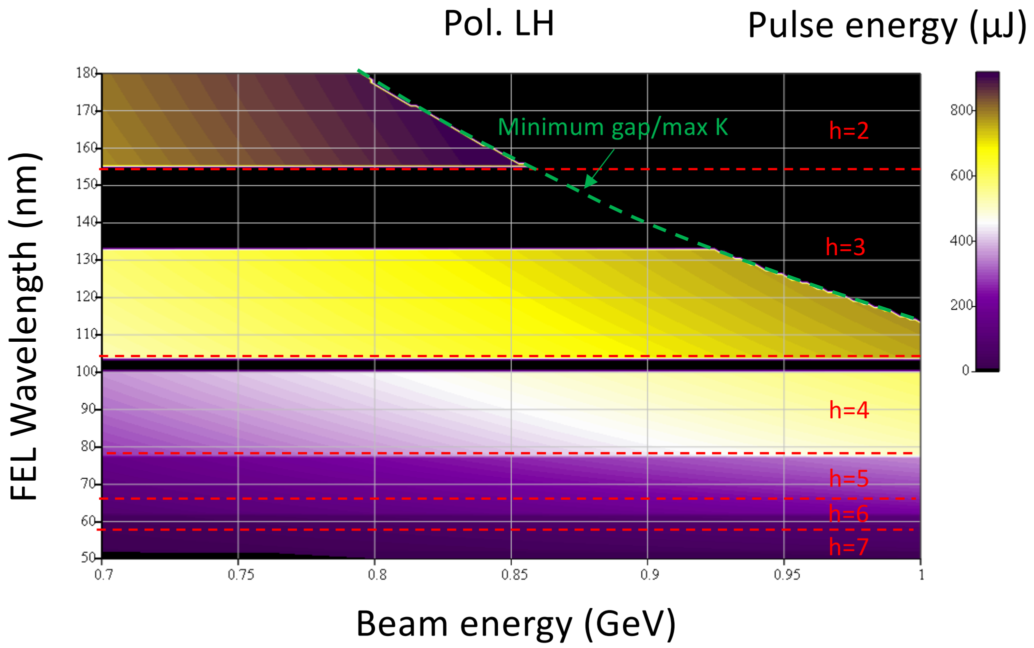

B: Seed range 600-800 nm

Continuous tuning in the range 60-180 nm

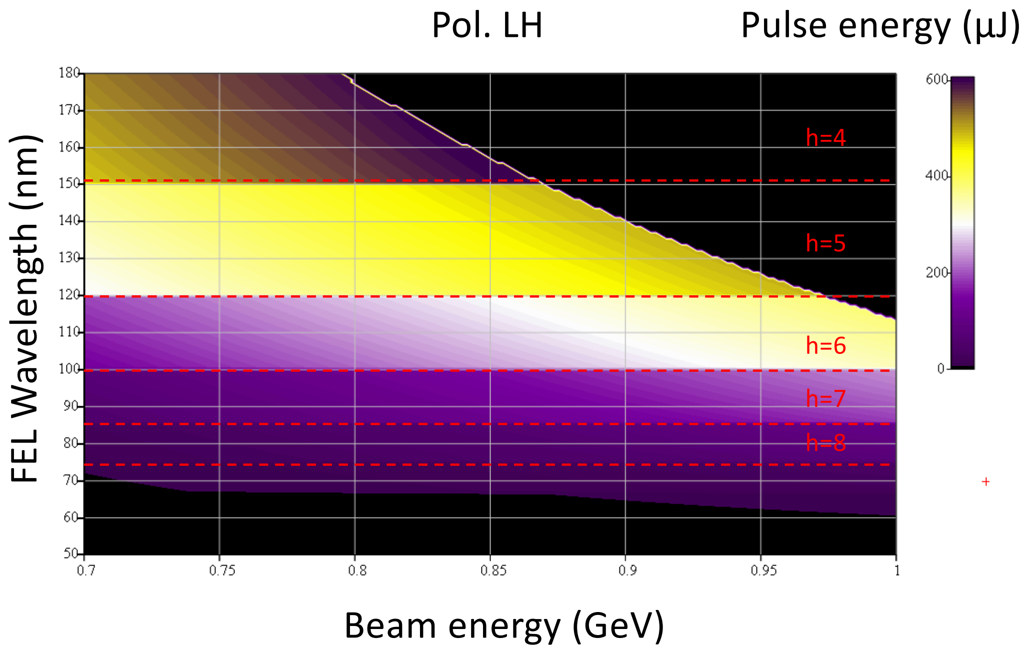

An OPA such as the TOPAS can seed the ARIA FEL line covering the spectral range 200-50 nm with a single OPA process 2HG (B). Improved performances below 100 nm can be achieved with the 4th HG process (A)

ARIA short summary

- ARIA operates in High Gain Harmonic Generation and may cover the VUV spectral range down to 50 nm with an undulator similar to the one of FERMI FEL-1. Contrary to FERMI it uses a seed longer than the electron bunch and uses the electron bunch shaping and control capabilities of Eupraxia@SPARCLAB for controlling thethe lught pulse properties.

- A commercial laser based on an Optical Parametric Amplifier such as the TOPAS should have the correct pulse energy and overall features to seed ARIA

- Two OPA regimes can be used to cover the full spectral range with harmonic order below seven. In case a single OPA regime is used with second harmonic conversion, the full range is covered with harmonic order below 12

AQUA

- Magnetic design & tuning range -> vacuum chamber geometry
- Longitudinal and transverse wake-fields
- Analysis of SABINA Undulator and first lessons for the AQUA undulator
  - **Magnetic:** field quality, field integrals, trajectory and FEL amplification
  - **Mechanical:** stability and reproducibility tests

Apple X magnetic design

Courtesy of A. Petralia

Modeling parameters:

- Remanent field Br = 1.35 T
- Undulator period λ_u = 18 mm
- 4 blocks / period, NdFeB
- # of periods (eff.) N = 110 (Lu=2m)

- Block sizes (mm): 18x18x4.4
- Min. gap = 1.5 mm
- **B_{max}=1 T / K_{max}=1.7**

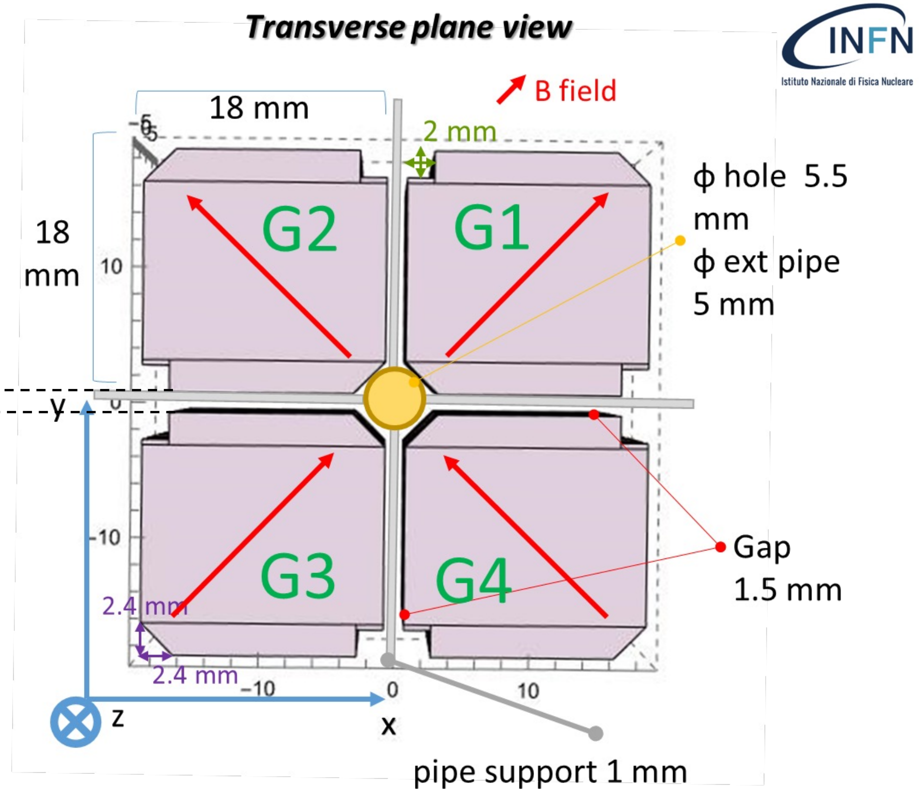

Number of periods N = 111.5

Total length of the magnetic array L_{und}= 1990.4 mm

End magnets

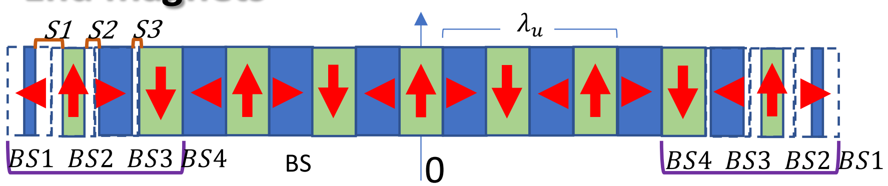

Optimized values for the end magnets: (mm)

Spaces:		Block sizes:
S1=0.1		BS1=1.1
S2=0.1	;	BS2=2.2
S3=0.1		BS3=2.4

Field Integrals

	LP (h)	CP	LP (v)	units
Ix	0	0	0	G m
Iy	0.0119	-0.0095	0.4118	G m
IIx	0	-0.0179	-0.1322	G m^2
IIy	0	-0.0001	0	G m^2

Undulator aperture

Courtesy of A. Petralia

Working parameters:

- Undulator period λ_u = 18 mm
- Min. gap = 1.5 mm
- Beam Energy = 1 GeV

Pipe ext. diam.	5 mm	5.5 mm	6 mm	6.5 mm	7 mm
Piper inner diam.	4 mm	4.5 mm	5 mm	5.5 mm	6 mm
Wedge cut (mm)	2.4	2.8	3.1	3.5	3.8
ϕ aperture (mm)	**5.515**	**6.081**	**6.505**	**7.071**	**7.495**
B max (T) (in LP)	1	0.94	0.87	0.80	0.75
K max (in LP)	1.7	1.57	1.47	1.35	1.26
K rms	1.2	1.11	1.04	0.95	0.89
max λ_0 (nm)	**5.79**	**5.25**	**4.9**	**4.5**	**4.23**
Negligible variation of the magnetic forces					

In each configuration the minimum gap is 1.5 mm -

Transverse plane view

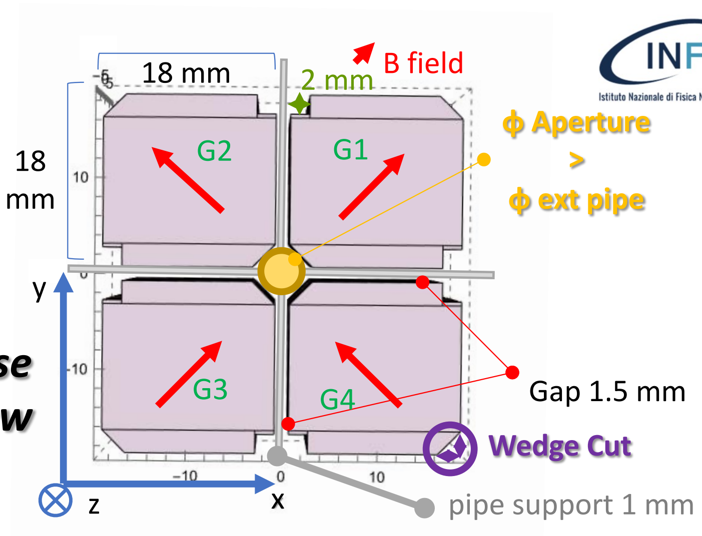

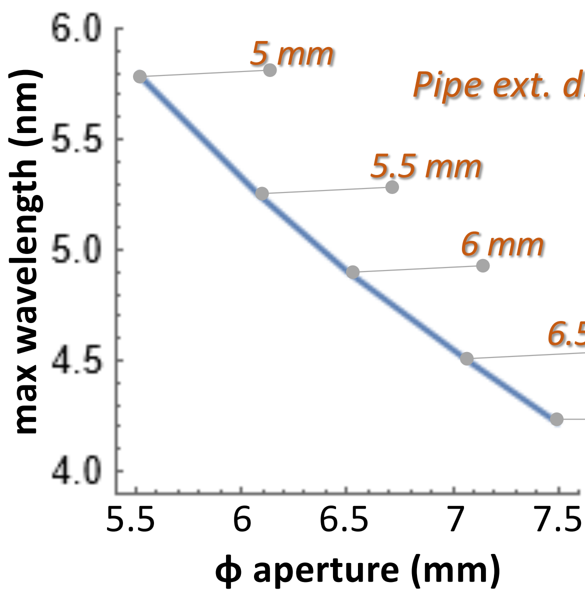

Increase tuning range: Shaped magnets with circular surface

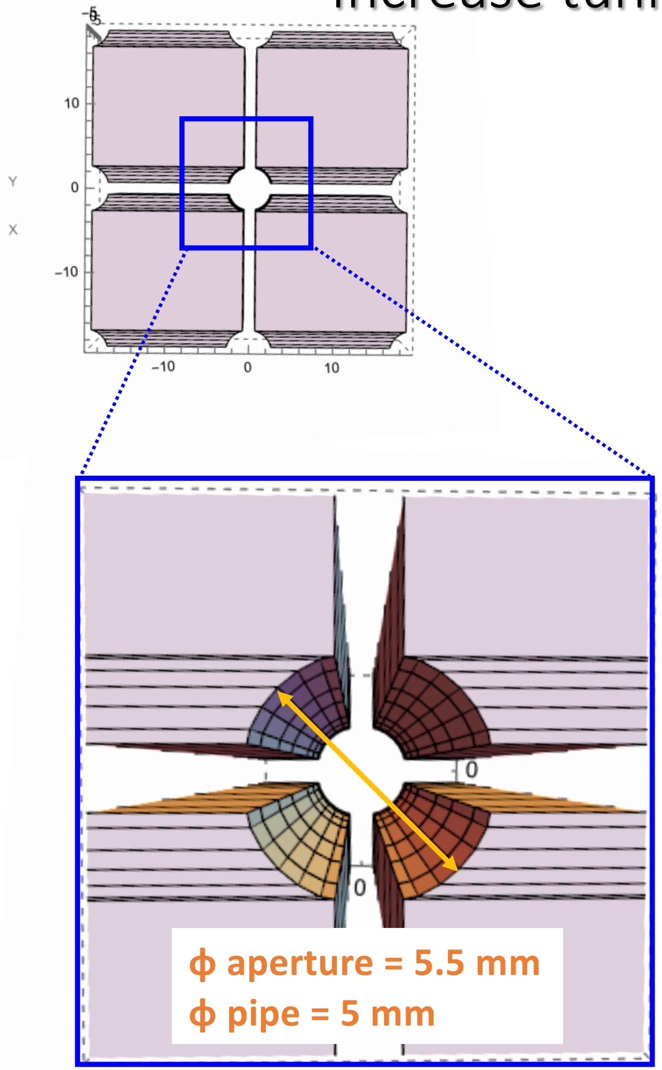

Pipe ext. diam.	5 mm	5.5 mm	6 mm	6.5 mm	7 mm
Pipe Int. diam.	4 mm	4.5 mm	5 mm	5.5 mm	6 mm
ϕ aperture (mm)	**5.5**	**6**	**6.5**	**7**	**7.5**
B max (T) (in LP)	1.04	0.97	0.91	0.85	0.79
K max (in LP)	1.75	1.63	1.53	1.42	1.32
K rms	1.24	1.16	1.08	1	0.93
max λ_0 (nm)	**5.95**	**5.49**	**5.08**	**4.72**	**4.4**

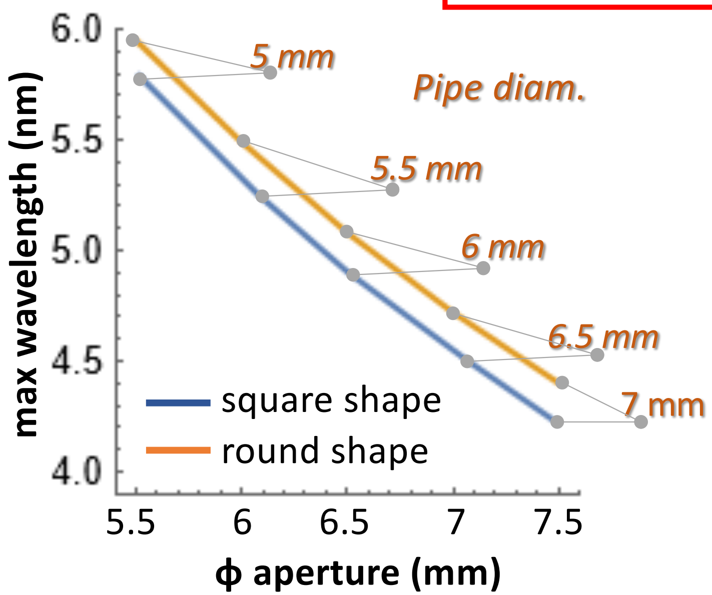

Results

Respect to the square shape case:

- Kmax increment +0.05 (3%)
- Max wl increment + 0.17 nm (3%)
- No improvement on the field homogeneity region (< 200 um from axis)
- Higher costs (?)

Vacuum pipe inner diameter

- Apple X undulator is symmetric, minimal access from sides. Vacuum chamber is a cylinder with sustaining blades of diameter d
- Wake fields mimimization requires smooth and regular surface – minimise apertures and other discontinuities
- Vacuum: access ports for pumping available only at the undulator transitions

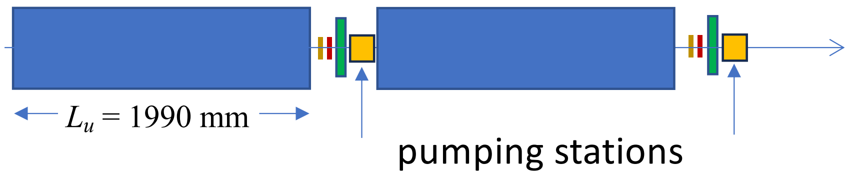

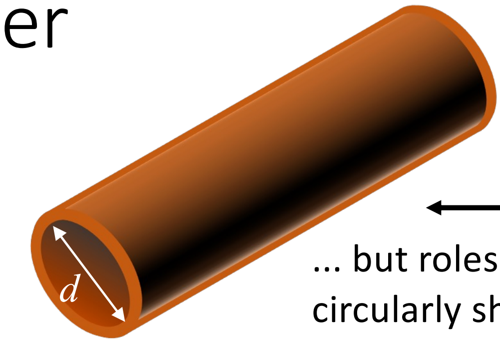

The square geometry could allow a thinner pipe wall

... but roles out the circularly shaped poles

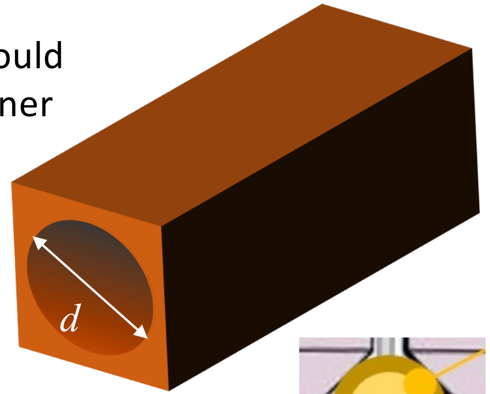

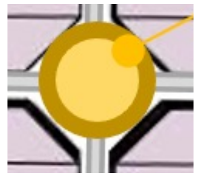

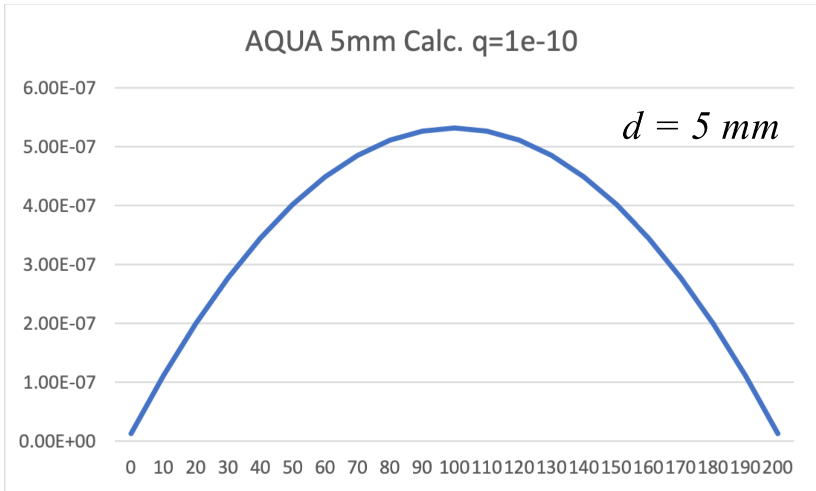

courtesy of A. Liedl

Longitudinal resistive wall wakefields

Courtesy of F. Nguyen

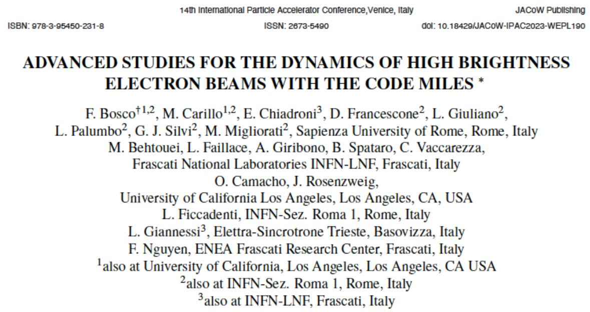

14th International Particle Accelerator Conference,Venice, Italy JACoW Publishing
ISBN: 978-3-95450-231-8 ISSN: 2673-5490 doi: 10.18429/JACoW-IPAC2023-WEPL190

ADVANCED STUDIES FOR THE DYNAMICS OF HIGH BRIGHTNESS ELECTRON BEAMS WITH THE CODE MILES *

F. Bosco†[1,2], M. Carillo[1,2], E. Chiadroni[3], D. Francescone[2], L. Giuliano[2],
L. Palumbo[2], G. J. Silvi[2], M. Migliorati[2], Sapienza University of Rome, Rome, Italy
M. Behtouei, L. Faillace, A. Giribono, B. Spataro, C. Vaccarezza,
Frascati National Laboratories INFN-LNF, Frascati, Italy
O. Camacho, J. Rosenzweig,
University of California Los Angeles, Los Angeles, CA, USA
L. Ficcadenti, INFN-Sez. Roma 1, Rome, Italy
L. Giannessi[3], Elettra-Sincrotrone Trieste, Basovizza, Italy
F. Nguyen, ENEA Frascati Research Center, Frascati, Italy
[1]also at University of California, Los Angeles, Los Angeles, CA USA
[2]also at INFN-Sez. Roma 1, Rome, Italy
[3]also at INFN-LNF, Frascati, Italy

Regardless of the external shape, from the inner side the vacuum chamber consists of a cylindrical Cu circular pipe of radius = 2 -> 3 mm

The energy loss due to the longitudinal resistive wall wakefields was calculated by M. Migliorati, F. Bosco *et al.* (Uni La Sapienza – Rome) and plugged into time dependent Genesis1.3 simulations for EuPRAXIA@SPARC_LAB electron both short and long bunches

Longitudinal wake effects: 30pC PWA"2μm" bunch

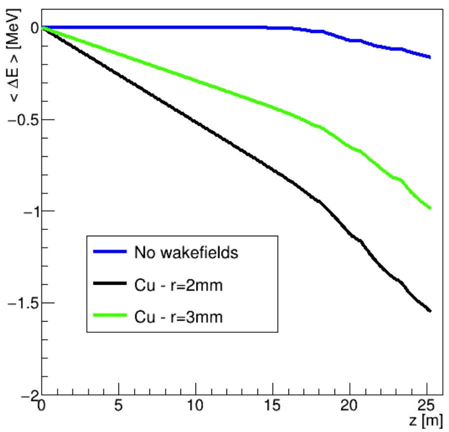

Average beam energy loss along the undulator

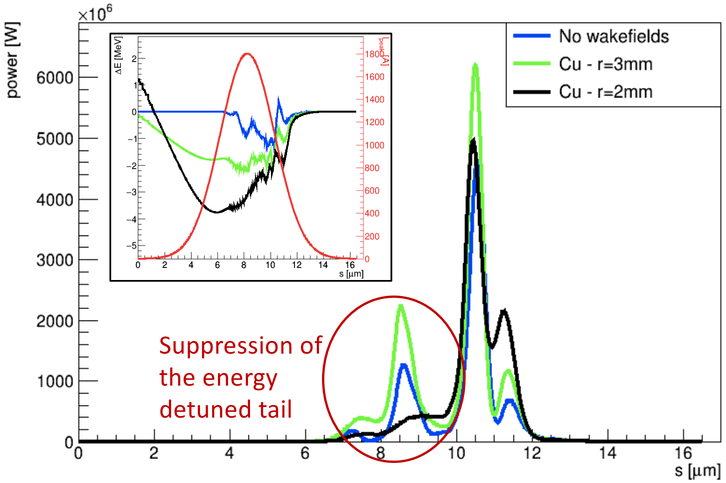

Energy loss (in the inset) and FEL output power at the exit of the undulators chain

Conclusion:

there is a negligible difference in the output power between no wakefields and longitudinal RW degradation at both inner radii for the short PWA bunch

Longitudinal wake effects – long bunch mode

Courtesy of F. Nguyen

Same analysis of the previous case, but for a 300 pC – 60 fs long bunch

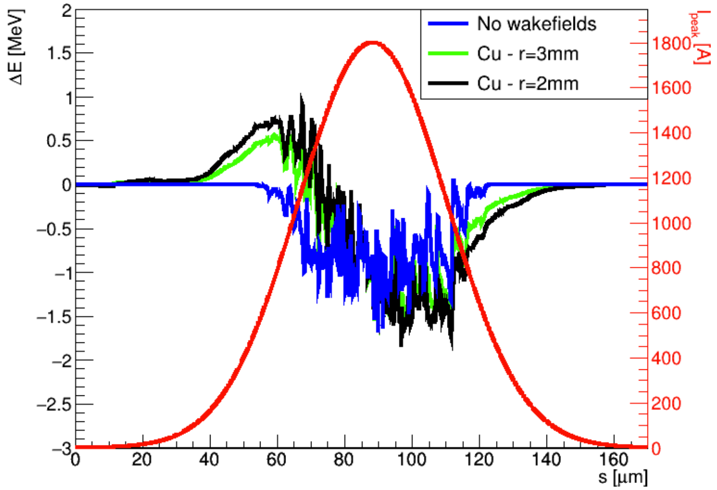

Average beam energy loss along the undulator

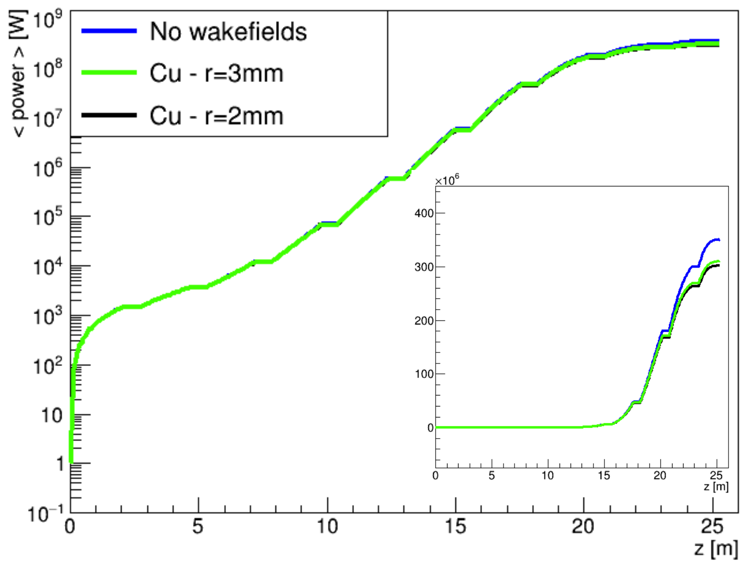

Average FEL output power in logarithmic scale along propagation coordinate (inset is the same in linear scale)

Conclusion: negligible difference in the energy loss (and so on the power growth) between no wakefields and longitudinal RW degradation at both inner radii

Transverse resistive wall wakefields

Courtesy of F. Nguyen

Transverse RW wakefields induced inside the cylindrical Cu vacuum chamber of radius *a*=2… 3 mm affect the electron bunch orbit along the undulator line, depending on the initial transverse offset at entrance.

Analytical treatment based on K. Bane & G. Stupakov formulae and the relationship between transverse and longitudinal RW impedances are used to estimate the kick angle κ_T parameter

$$W_t(s) = \frac{2}{a^2}\int_0^s W_\ell(s')\mathrm{d}s', \quad Z_t(k) = \frac{2}{a^2}\frac{Z_\ell(k)}{k}$$

$$W_z(s) = \frac{Z_0 c}{\pi a^2} e^{-s/4c\tau} \cos\left[\sqrt{\frac{2\omega_p}{ac}} s\right]$$

$$\varkappa_T = \frac{\text{kick angle [rad]}}{\text{unit path length [m]} \times \text{unit vertical offset [m]}}$$

short 2 μm bunch

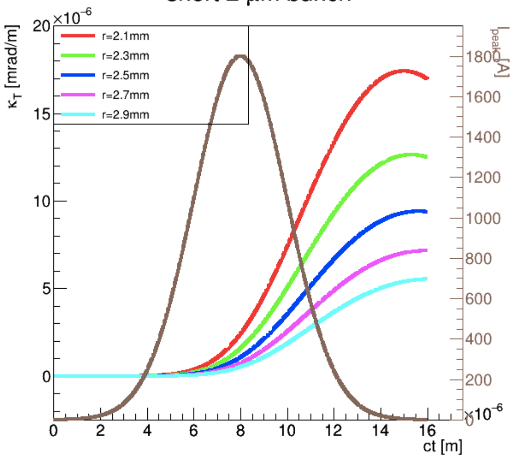

long 20 μm bunch

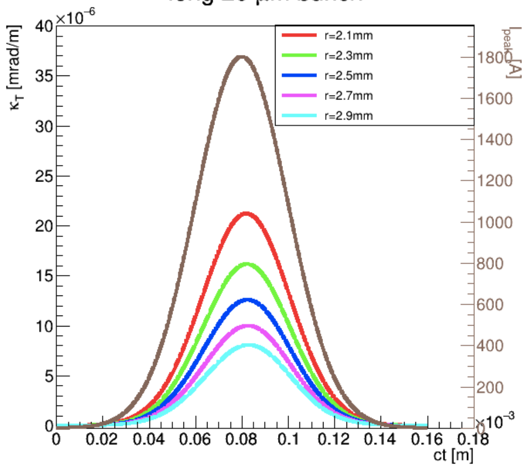

Preliminary conclusions

Short bunch: Max kick: 2×10^{-5} mrad/m but outside the current peak

Long bunch: same order of magnitude, but superimposed to the current profile

Sensitivity to transverse offsets (2 μm bunch), no wakes

Courtesy of F. Nguyen

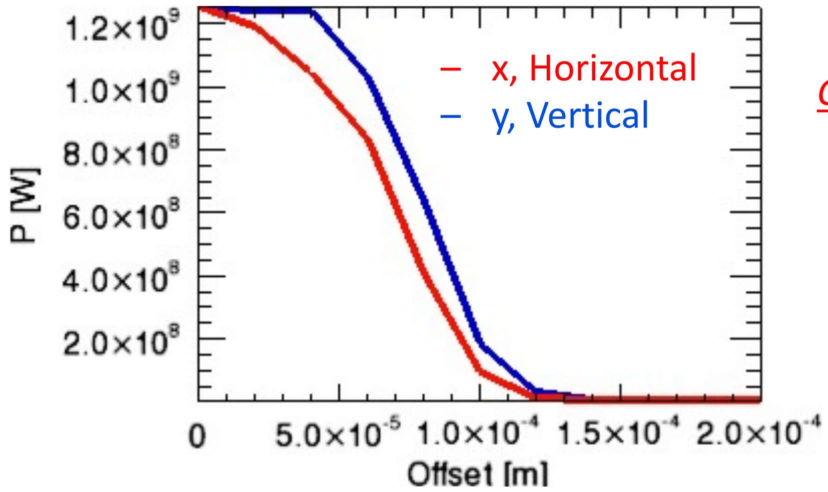

FEL power reduction in
Circular polarization APPLE-X

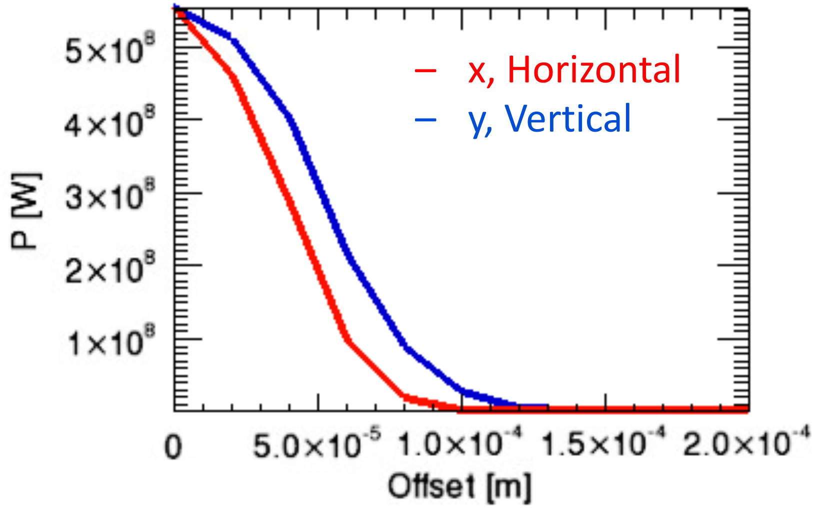

FEL power reduction in
Linear polarization APPLE-X

Conclusion

Circular Polarization: 50μm offset gives rise to ~ 67% power decrease
Linear Polarization: the reduction is steeper and 50μm is probably too much

EUPRAXIA Undulator Model (Courtesy of Mario Del Franco)

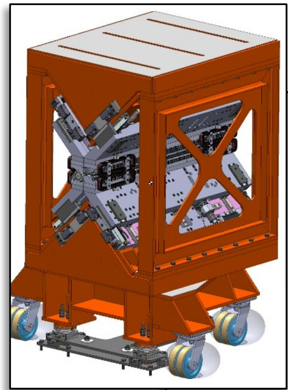

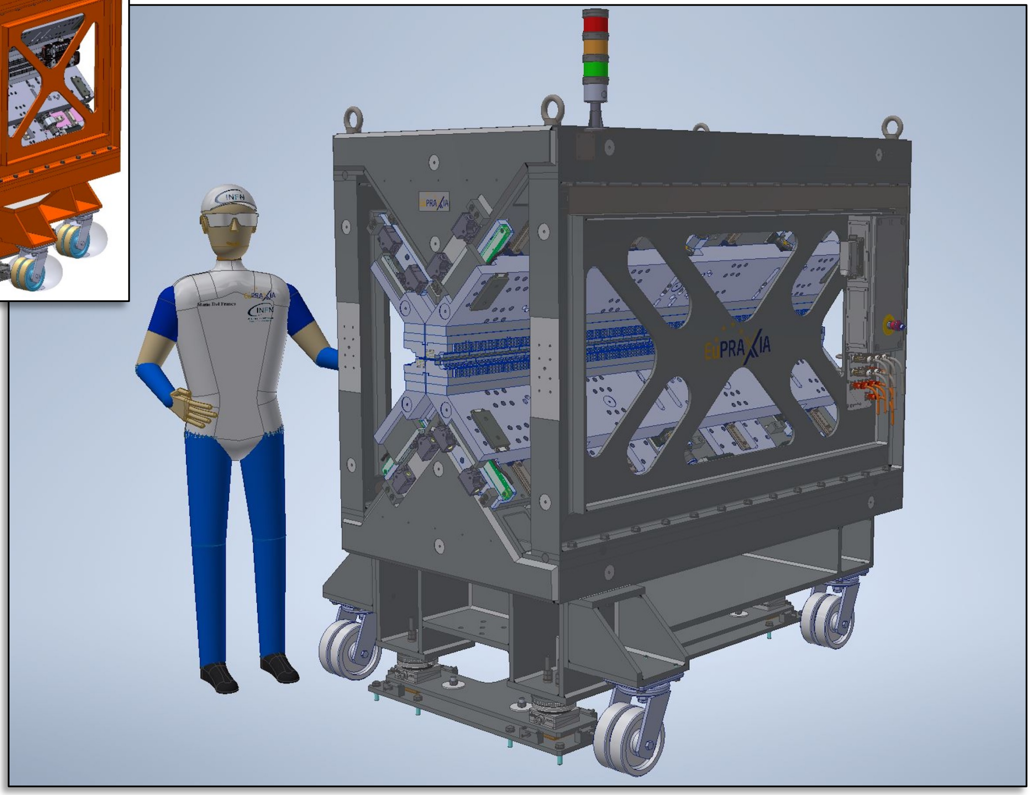

Mechanical model derived from SABINA Undulator model:

SABINA: built by ***KYMA*** *(*2022-2023), APPLE-X 1300 mm long modules, period 5.5 cm – 10 mm aperture

AQUA - APPLE-X 1990 mm long modules, period 18 mm, polarization circular left, circular right, linear horizontal, linear vertical.

From SABINA Undulator:

- Magnetic measurements
- Mechanical measurements

Field errors distribution, from the SABINA undulator

1st SABINA module, measured by Kyma. Analysis by A. Petralia

For Circular Pol. mode (phase 13.75 mm), @ minimum gap 5 mm, **on axis field components** (red B_x, blue B_y, green B_z)

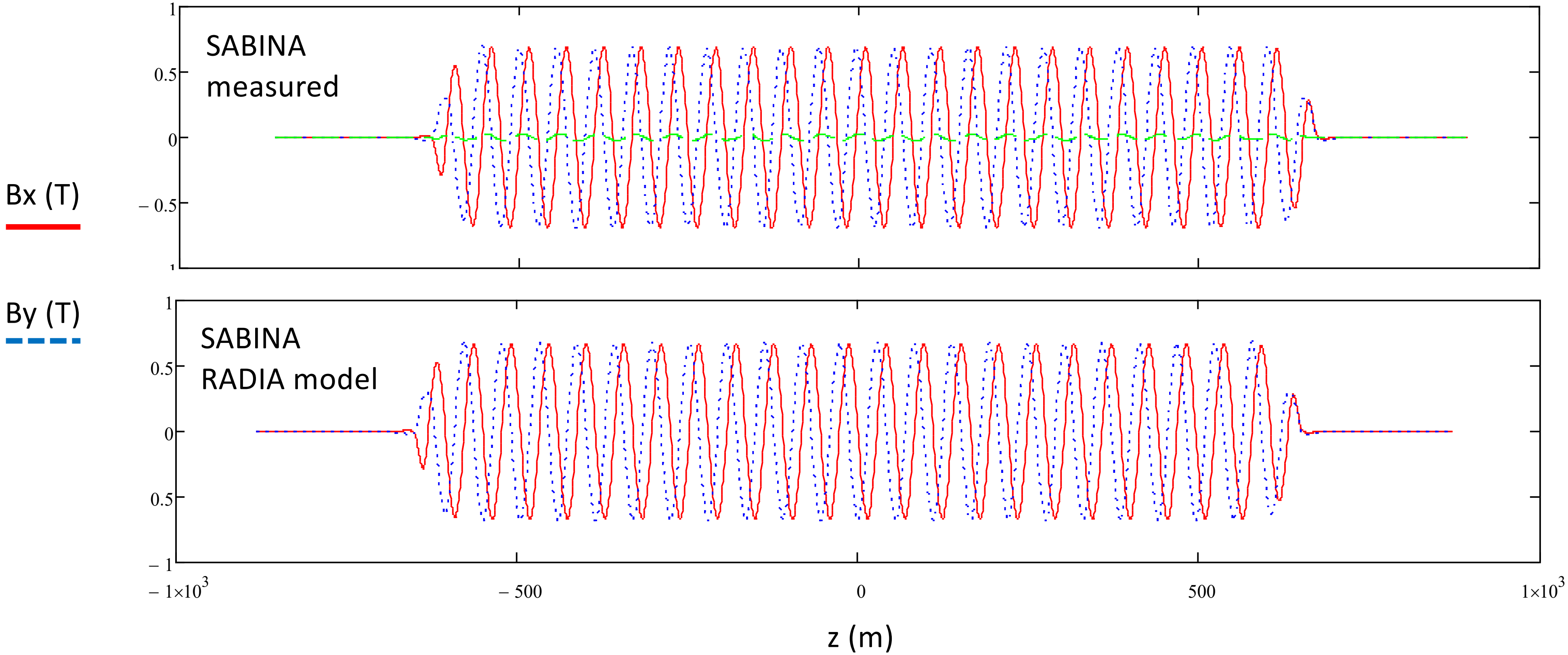

Difference between Kyma measure and RADIA model,

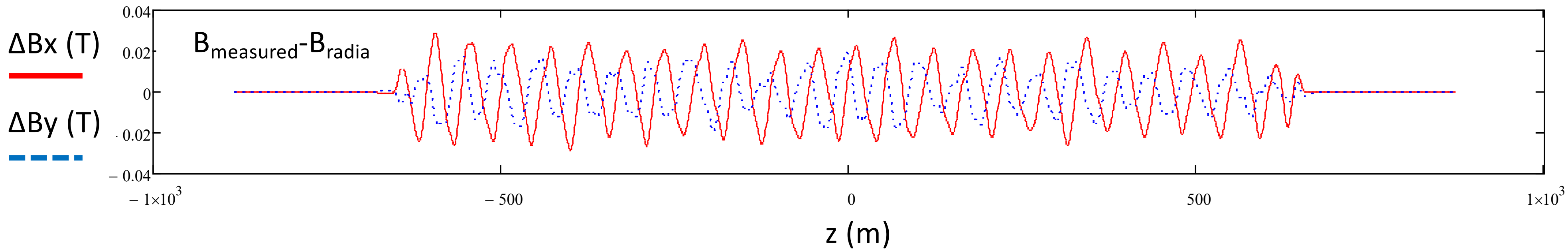

The effective peak field in the real undulator (K_{rms}=3.529) is higher than in the Radia model (K_{rms}=3.453)

Rescaling in RADIA the remanent field of the magnets to have same peak field of the Kyma device (at min gap)

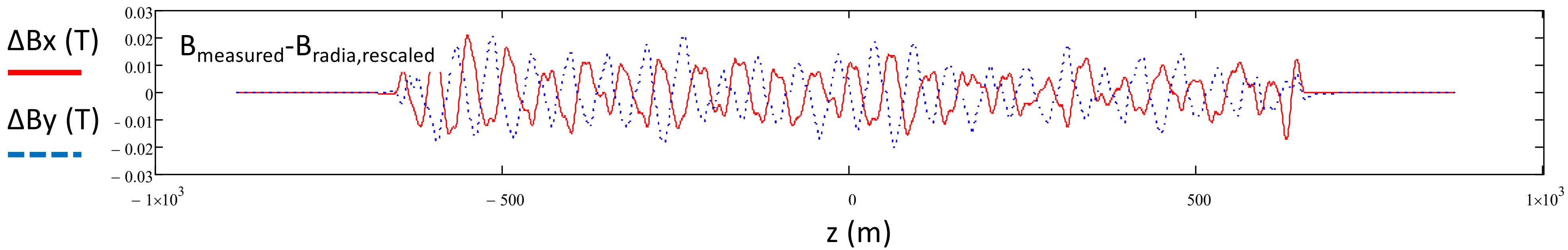

The difference gives an estimate of the deviation from the ideal field (peak < 2%). We calculate the field integral on each half period, rescale this value to the AQUA period length (about 1/3 of the SABINA period) and we used this sequence of "first field integrals" to estimate the FEL performance of AQUA with a more realistic field distribution.

First tolerance study of undulator magnetic field errors for the AQUA beamline using the data from the SABINA undulator measurements.

Courtesy of M.Opromolla

- Considered a simulation in a **long bunch case to reduce SASE shot to shot statistical fluctuations**
- Magnetic field errors **reconstructed from the SABINA undulators measurements** (3 modules used in random sequence to provide similar field integrals)
- Without orbit correction the beam walks out of axis and particles are lost.
- **Added correctors at the end of each undulator** section to **zero the second field integral betweenthe undulators** (similar to the correction of a trajectory feedback system)

Long beam (60 fs), ρ_{3d} = 0.94e-3

E (GeV)	1	σ_E slice (MeV)	0.489
Q (pC)	200	$\varepsilon_{x,y}$ slice (um)	0.8
I_{peak} (kA)	1.26	$\sigma_{x,y}$ (µm)	60.9, 56

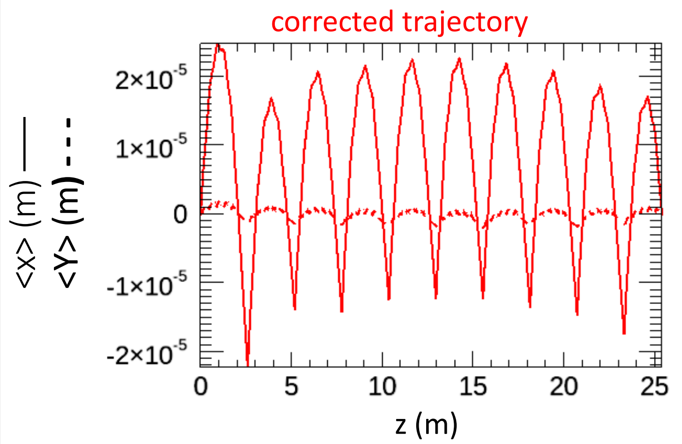

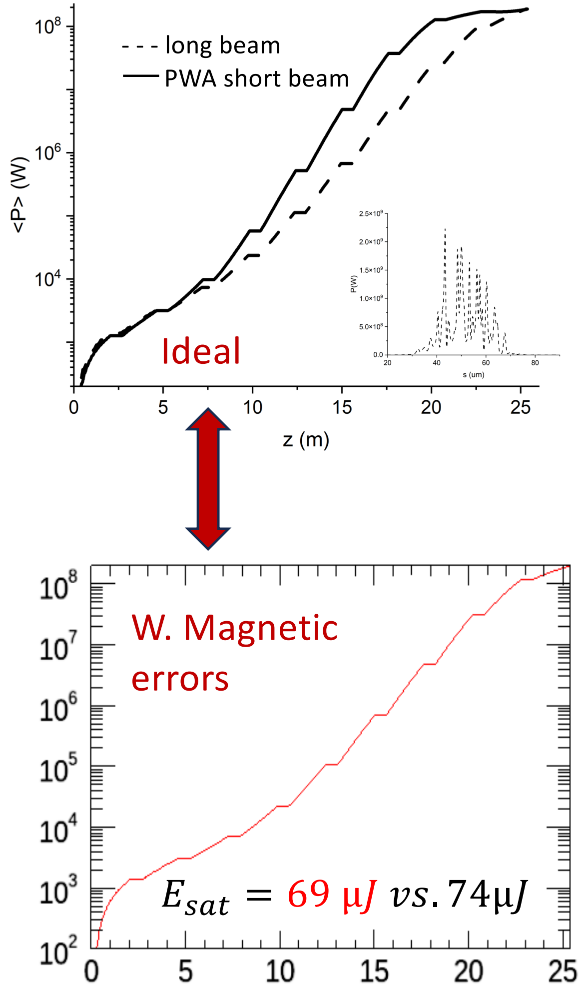

First and second field integrals specs. achieved for the SABINA undulator seems sufficient for the AQUA undulator line

Mechanical stress analysis of the SABINA undulator

- We are verifying the stability and reproducibility of the mechanical structure of the SABINA undulator
- In collaboraton with the **Holographyc Interferometry & Fibre Optic Sensors (HIFOS) Laboratory at *ENEA*** (ref. M. Caponero) we are measuring the deformations of the undulator guilders
- The technique:
  - A diffraction grating is produced by modifying the refraction index of the core of a fiber (FBG Sensors). Rough approximation: the refractive index has a sinusoidal modulation along the axis of the fibre.
  - the sensor length is 10 mm, temperature and strain sensing at the level 0.1K - $1/10^6$ relative elongation sensitivity
  - Many sensors can stay chained along one single fiber for quasi-distributed measurements
- Can be implemented for:
  - Characterization of mechanical deformations
  - Characterization of local magnetic field, but ... no sensitivity to e.m. fields (spectroscopic measurement)

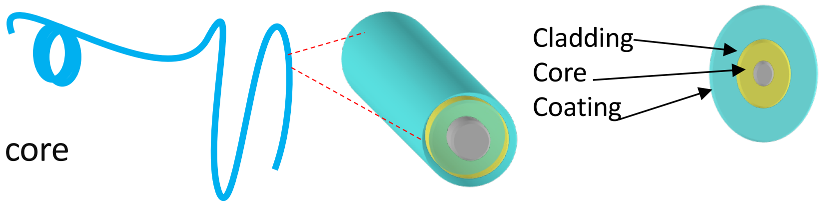

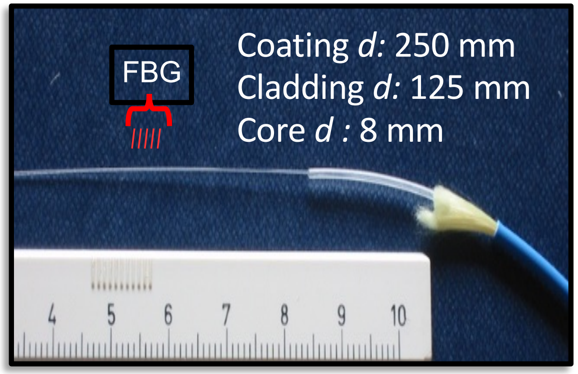

SABINA Undulator stress analysis

Courtesy of I. Balossino, A. Selce, A. Polimadei, A. Vannozzi, M. Del Franco, L. Sabbatini, M. Caponero

deformations in µm

CAD model by KYMA

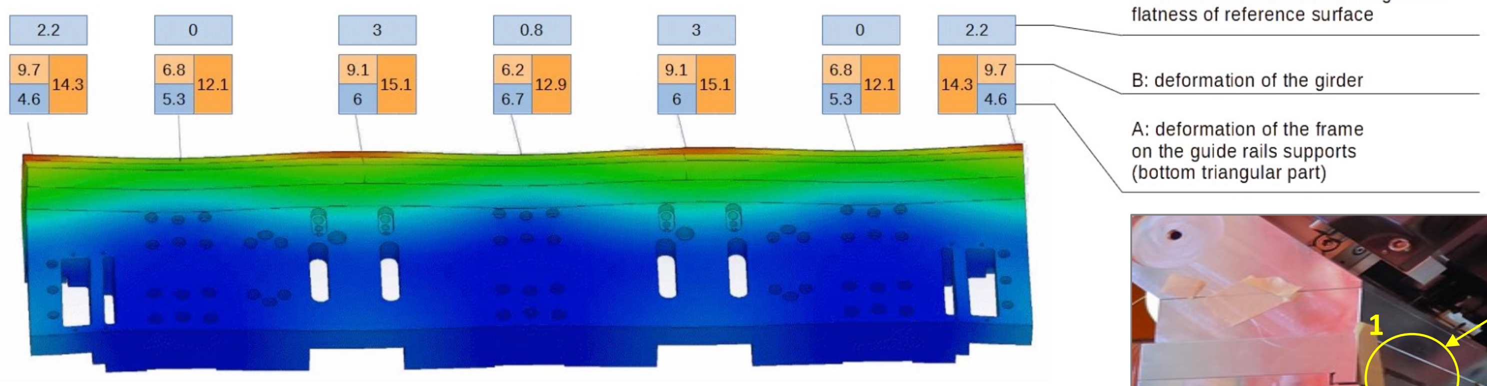

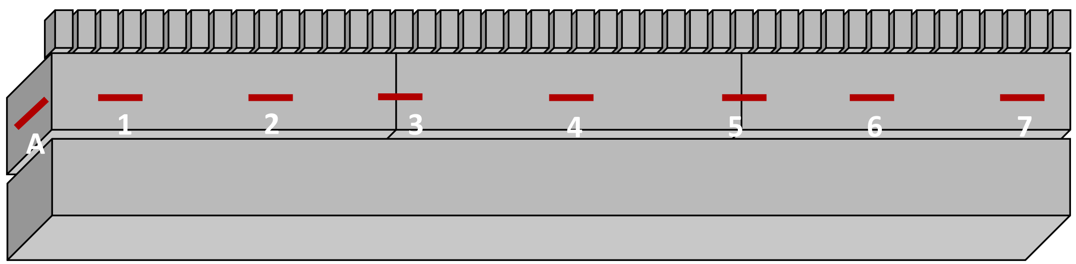

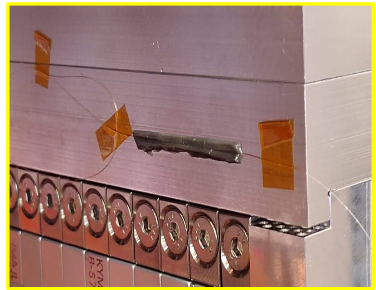

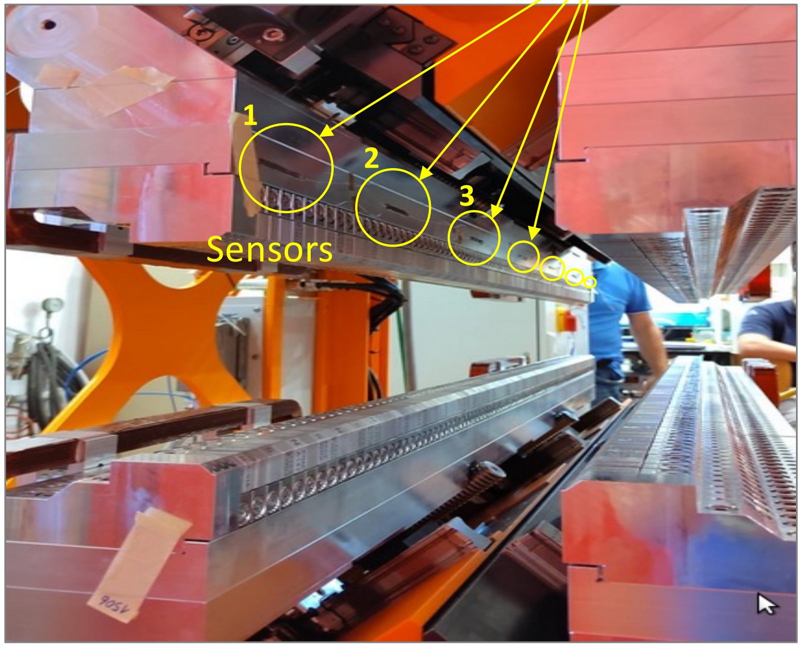

Preliminary results

Units are in wavelength shift Δλ. Δλ = 150 pm corresponds to 10^{-4} relative change in length (strain).

A Temperature monitor. The background trend is related to temperature drifts

Opening and closing the undulator gap between 5mm and 150 mm we observe:

- sensors 3 & 5 on the gaps show a substantially larger deformation (15x to 30x) with respect to the others installed on the solid bulk bars
- The behavior is not symmetric: sensor 3 and sensor 5 show an opposite behavior
- Relaxation during movements on sensor 6

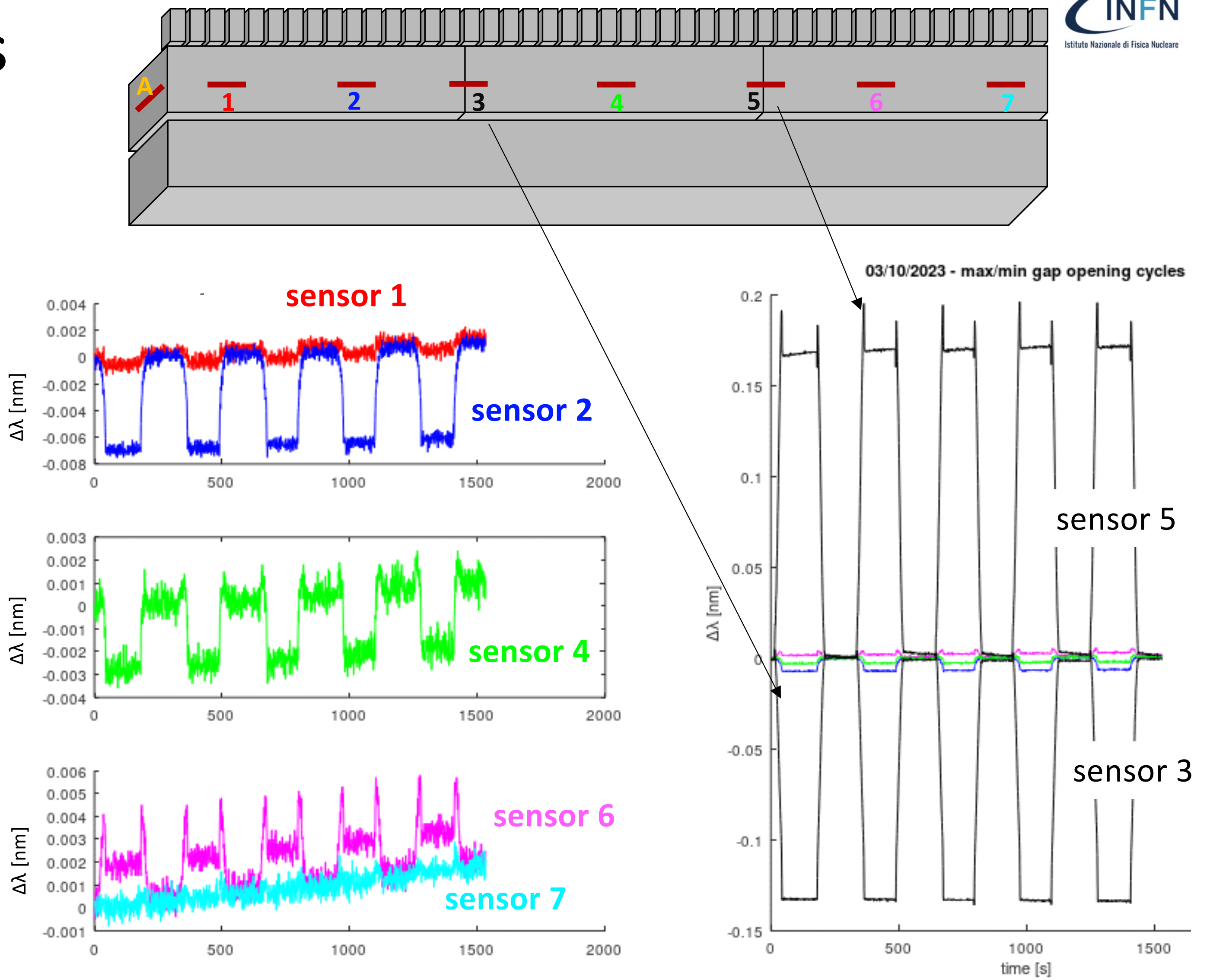

AQUA summary

- Magnetic design is completed for different magnet apertures. The effective aperture depends on the next item
- Vacuum chamber design is in progress. Diameter between 5 and 6 mm. The diameter in this range still allows 20% photon energy tuning via gap aperture change
- Longitudinal wake fields do not constitute a problem for the pipe radius/beam conditions selected
- Transverse wake field calculations were carried out. The figures will be used to define the straightness and alignment tolerances required by the vacuum chamber.
- The tolerance on the beam injection indicates that the transverse beam position jitter at the undulator entrance has to be less than 50 um pp. Similar simulations will be carried out for the injection angle jitter.
- Similar calculation are in progress for the determination of the maximum field integral from the undulator and from the quadrupoles alignement.
- Mechanical stiffness of the SABINA undulator is indicating some unexpected behavior under investigation. The results will be discussd with the producer to explore mitigation strategy for the AQUA undulator.

LIDAR 3D Scanner – Views of the SABINA Module

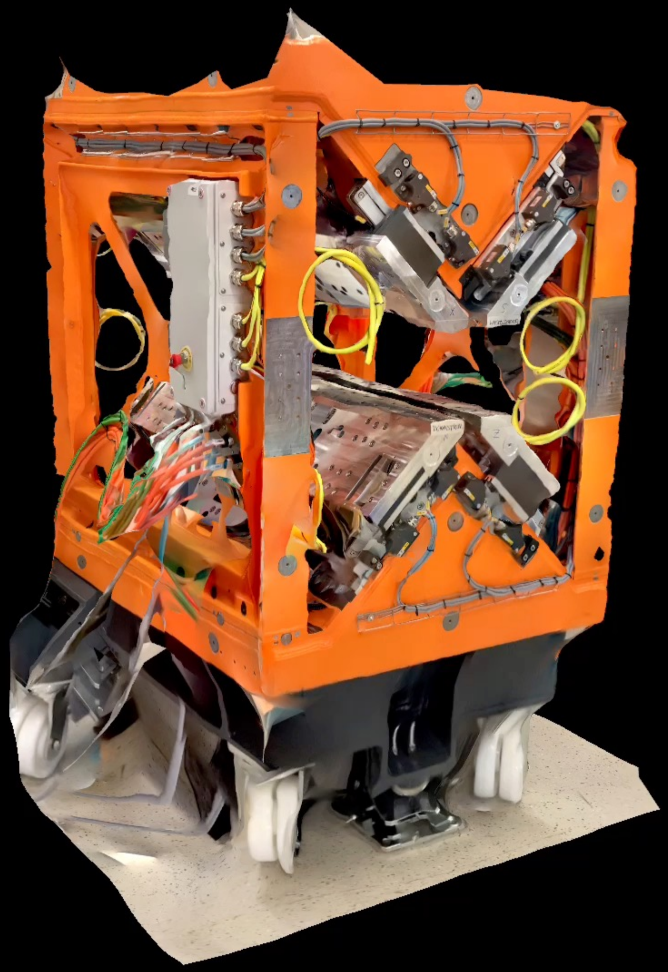

Timeline for SCU development at FERMILAB
(Courtesy of C. Boffo)

Some delay wr. to previous schedule.
New schedule:

- Prototype completed (testing after Christmas 23')
- Vacuum vessel in final stages of manufacturing
- Thermal shield and MLI in procurement
- Assembly will be completed in September 2024

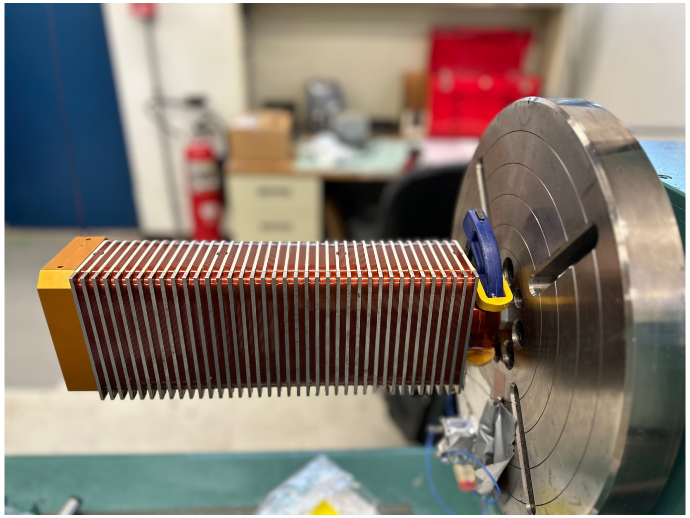

ROADMAP	2023 Q4	2024 Q1	2024 Q2	2024 Q3	2024 Q4
Prototyping	Test				
Design	Complete coil design Complete beampipe design Ancillaries design				
Coil manufacturing		Component procurement	Coil manufacturing		
System assembly	Component procurement			Assembly	Test
Dissemination			Participation to conferences and workshops		